

Model-independent estimates for the Abelian Z' boson at modern hadron colliders

Alexey Gulov* and Andrey Kozhushko†

Dnipropetrovsk National University, Dnipropetrovsk, Ukraine

February 24, 2024

Abstract

The model-independent constraints on the Abelian Z' couplings from the LEP data are applied to estimate the Z' production in experiments at the Tevatron and LHC. The Z' total and partial decay widths are analyzed. The results are compared with model-dependent predictions and present experimental data from the Tevatron. If we assume the 1-2 σ hints from the LEP data to be a signal of the Abelian Z' boson, then the Tevatron data constrain the Z' mass between 400 GeV and 1.2 TeV.

1 Introduction

Searching for signals of new physics beyond the standard model (SM) is an essential part of experiments at modern colliders. New phenomena could be discovered through deviations of observed quantities from the predicted SM background. However, observables in experiments at hadron colliders can be calculated with significant theoretical uncertainties coming mainly from the parton distribution functions of initial states and complicated structure of hadronic final states. In this situation one can only hope to discover the most prominent signals in the most clear processes. This is the reason to pay attention to searching for resonances of new heavy particles decaying into lepton pairs.

A neutral vector boson (Z' boson) is probably the most perspective intermediate state in scattering processes of quarks and leptons which could be discovered in the Tevatron and LHC experiments. At the parton level it appears in the annihilation channel, its mass is allowed to be of order 1 TeV by current experimental constraints, and it is a necessary component of popular grand unification theories and other models with extended gauge sector (see [1, 2, 3] for review).

In general, the accurate description of Z' resonance requires to consider scattering amplitudes with intermediate virtual states. But if the resonance is a narrow one, then it can be described in a more simple way by a small number of convenient characteristics of the production and the decay of the particle. In this approach it is enough to set the Z' mass and width, the production cross-section, and the branching ratio into the final state. Supposing some numbers

*gulov@dsu.dp.ua

†a.kozhushko@yandex.ru

for the Z' parameters in various estimates one could and, in principle, would take into account all the available experimental constraints on Z' from previous experiments.

Of course, effects of Z' boson can be calculated in details for each specific model beyond the SM. Such estimates are widely presented in the literature [4, 5, 6]. Some set of popular E_6 based models and left-right models is usually considered in this approach. However, probing the set we can still miss the actual Z' model. In this regard, it is useful to complement model-dependent Z' searching by some kind of model-independent analysis, i.e. the analysis covering a lot of models. Almost all of the usually considered models belong to the models with so-called Abelian Z' boson. In Ref. [7, 8] we found the relations which hold in any model containing the Abelian Z' boson and satisfying the following conditions:

- only one neutral vector boson exists at energy scale about 1-10 TeV,
- the Z' boson can be phenomenologically described by the effective Lagrangian [1, 2, 3] at low energies,
- the Z' boson and other possible heavy particles are decoupled at considered energies, and the theory beyond the Z' decoupling scale is either one- or two-Higgs-doublet standard model (THDM),
- the SM gauge group is a subgroup of possible extended gauge group of the underlying theory. So, the only origin of possible tree-level Z' interactions to the SM vector bosons is the Z - Z' mixing.

These relations cover almost all of the usually considered set of models (see [9, 10] for details). They require the same Z' couplings to the left-handed fermion currents within any SM doublet and the universal absolute value of the Z' couplings to the axial-vector currents for all the massive SM fermions. The relations reduce significantly the number of unknown Z' parameters. This allows to constrain the parameters by existing experiments as well as to predict the quantities used in the analysis of the Tevatron and LHC experiments.

Recently we summarized the information about Z' couplings to leptons and quarks which can be extracted from the LEP experiments [9, 10]. The Z' coupling to axial-vector currents was constrained by both LEP I and LEP II $\mu^+\mu^-$, $\tau^+\tau^-$ data. In different processes it shows hints at about 1σ confidence level (CL) with the approximately same maximum-likelihood (ML) value. This value can be used in estimates of observables in the Tevatron and LHC experiments. As for the couplings to vector currents, the Z' coupling constant to electron can be constrained by the LEP II e^+e^- data only. Although the backward scattering shows a signal at the 2σ CL, the ML value is outside of the 95% CL interval calculated by the complete set of bins. In this situation we refrain from using that ML value in our estimates. Nevertheless, the vector coupling is constrained at 95% CL. The upper bound on the electron vector coupling agrees closely with the corresponding upper bound on the axial-vector coupling. This fact allows us to suppose the rest of vector couplings to be constrained by the same value, since no evident signals were discovered in other scattering processes measured by the LEP collaborations. It is worth to note that all the conclusions derived from the LEP data are also valid if one considers the THDM as the low-energy theory instead of the usual minimal SM.

The main goal of the present paper is to obtain estimates for the Z' parameters used in searching for the narrow resonance by applying the LEP constraints on the Z' couplings. Both the minimal SM and the THDM will be considered as the low-energy theory.

The paper is organized as follows. Sec. 2 contains a necessary information about Z' interactions at low energies, the relations between the Z' couplings and the limits on these couplings obtained from the LEP data. In Sec. 3 the Z' production cross-section at hadron colliders is estimated. The bounds on the total and partial decay widths are presented in Sec. 4. In Sec. 5 we discuss the application of our results comparing them, in particular, with the Tevatron experimental data and model-dependent predictions for the Tevatron and LHC. The explicit Lagrangian used for the calculations is given in Appendix A.

2 Theoretical and experimental constraints on the Z' couplings

In this paper we discuss mainly the Z' couplings to the vector and axial-vector fermion currents described by the Lagrangian

$$\begin{aligned}\mathcal{L}_{Z\bar{f}f} &= \frac{1}{2}Z_\mu\bar{f}\gamma^\mu[(v_{fZ}^{\text{SM}} + \gamma^5 a_{fZ}^{\text{SM}})\cos\theta_0 + (v_f + \gamma^5 a_f)\sin\theta_0]f, \\ \mathcal{L}_{Z'\bar{f}f} &= \frac{1}{2}Z'_\mu\bar{f}\gamma^\mu[(v_f + \gamma^5 a_f)\cos\theta_0 - (v_{fZ}^{\text{SM}} + \gamma^5 a_{fZ}^{\text{SM}})\sin\theta_0]f,\end{aligned}\quad (1)$$

where f is an arbitrary SM fermion state; a_f and v_f are the Z' couplings to the axial-vector and vector fermion currents; θ_0 is the Z - Z' mixing angle; v_{fZ}^{SM} , a_{fZ}^{SM} are the SM couplings of the Z -boson. Such a parametrization is suggested by a number of natural conditions. First of all, the Z' interactions of renormalizable types are to be dominant at low energies $\sim m_W$. The non-renormalizable interactions generated at high energies due to radiation corrections are suppressed by the inverse heavy mass $1/m_{Z'}$ (or by other heavier scales $1/\Lambda_i \ll 1/m_{Z'}$) and therefore at low energies can be neglected. It is also assumed that the Z' is the only neutral vector boson with the mass $\sim m_{Z'}$.

It is obvious that the Lagrangian (1) requires the Z' boson to enter the theory as a gauge field through covariant derivatives with a corresponding charge. This idea allows also to introduce Z' couplings to SM scalar and vector fields. Although the latter couplings are inessential in the analysis of the Z' production cross-section in fermion collisions, they contribute to the Z' width. We assume that the $SU(2)_L \times U(1)_Y$ gauge group of the SM is a subgroup of the GUT group. In this case, a product of generators associated with the SM subgroup is a linear combination of these generators. As a consequence, all the structure constants connecting two SM gauge bosons with Z' have to be zero. Hence, the Z' interactions to the SM gauge fields at the tree level are possible due to a Z - Z' mixing only.

We will consider both the SM and the THDM as the low-energy theory. The explicit Lagrangian describing Z' couplings to the SM fields can be found in Appendix A.

The parameters a_f , v_f , and θ_0 must be fitted in experiments. In a particular model, one has some specific values for them. In case when the model is unknown, these parameters remain potentially arbitrary numbers. In most

investigations they are usually considered as independent ones. However, this is not the case if one assumes that the underlying extended model is a renormalizable one. In Refs. [7, 8] it was shown that these parameters are correlated as

$$v_f - a_f = v_{f^*} - a_{f^*}, \quad a_f = T_{3f} \tilde{g} \tilde{Y}_\phi, \quad (2)$$

where f and f^* are the partners of the $SU(2)_L$ fermion doublet ($l^* = \nu_l, \nu^* = l, q_u^* = q_d$ and $q_d^* = q_u$), T_{3f} is the third component of weak isospin, and $\tilde{g} \tilde{Y}_\phi$ determines the Z' interactions to the SM scalar fields (see Appendix for details). The parameter $\tilde{g} \tilde{Y}_\phi$ defines also the Z - Z' mixing angle in (1).

As it was discussed in [9, 10], the relations (2) cover a popular class of models based on the E_6 group (the so called LR, χ - ψ models) and other models, such as the Sequential SM [11]. Thus, they describe correlations between Z' couplings for a wide set of models beyond the SM. That is the reason to call the relations model-independent ones.

The couplings of the Abelian Z' to the axial-vector fermion current have a universal absolute value. The value is proportional to the Z' coupling to scalar fields. Then, the Z - Z' mixing angle θ_0 can be also determined by the axial-vector coupling.

At low energies the Z' couplings enter the cross-section together with the inverse Z' mass, so it is convenient to introduce the dimensionless couplings

$$\bar{a}_f = \frac{m_Z}{\sqrt{4\pi m_{Z'}}} a_f, \quad \bar{v}_f = \frac{m_Z}{\sqrt{4\pi m_{Z'}}} v_f, \quad (3)$$

which are constrained by experiments. Since the axial-vector coupling is universal, we will use the notation

$$\bar{a} = \bar{a}_d = \bar{a}_{e^-} = -\bar{a}_u = -\bar{a}_\nu. \quad (4)$$

Then the Z - Z' mixing is

$$\theta_0 \approx -2\bar{a} \frac{\sin \theta_W \cos \theta_W}{\sqrt{\alpha_{\text{em}}}} \frac{m_Z}{m_{Z'}}. \quad (5)$$

It also follows from (2) that for each fermion doublet only one vector coupling is independent:

$$\bar{v}_{fd} = \bar{v}_{fu} + 2\bar{a}. \quad (6)$$

As a result, Z' couplings can be parameterized by seven independent constants \bar{a} , \bar{v}_u , \bar{v}_c , \bar{v}_t , \bar{v}_e , \bar{v}_μ , \bar{v}_τ .

Recently we obtained limits on Z' couplings from the LEP I and LEP II data [9, 10]. We found some hints of Z' boson at 1-2 σ CL. Namely, the constants \bar{a} and \bar{v}_e show non-zero ML values. The axial-vector coupling \bar{a} can be constrained by the LEP I data (through the mixing angle) and by the LEP II $e^+e^- \rightarrow \mu^+\mu^-$, $\tau^+\tau^-$ data. The corresponding ML values are very close to each other. This value

$$\bar{a}^2 = 1.3 \times 10^{-5} \quad (7)$$

will be used in our estimates. The 95% CL interval was also obtained by the experimental data:

$$0 < \bar{a}^2 < 3.61 \times 10^{-4}. \quad (8)$$

The electron vector coupling \bar{v}_e can be constrained by the LEP II $e^+e^- \rightarrow e^+e^-$ data. An evident non-zero ML value occurred in fits taking into account the backward scattering bins only. Those fits showed 2σ signal of the Z' boson. On the other hand, that ML value was excluded at 95% CL by fits including all the bins. This instability is the reason to refrain from using the ML value of \bar{v}_e in our estimates. The 95% CL interval on \bar{v}_e will be taken into account only:

$$4 \times 10^{-5} < \bar{v}_e^2 < 1.69 \times 10^{-4}. \quad (9)$$

Other Z' coupling constants cannot be severely constrained by existing data. Among them \bar{v}_u , \bar{v}_c , and \bar{v}_μ play an important role in the process $q\bar{q} \rightarrow Z' \rightarrow \mu^+\mu^-$ which is most perspective to discover the Z' resonance. Taking into account that no evident signals of new physics were found by the LEP collaborations in the processes involving quarks, muons and tau-leptons, we constrain the values of \bar{v}_u , \bar{v}_c , \bar{v}_t , \bar{v}_μ , and \bar{v}_τ by the widest interval from the 95% CL intervals for \bar{a} and \bar{v}_e :

$$0 < \bar{v}_{\text{other } f}^2 < 4 \times 10^{-4}. \quad (10)$$

The knowledge of possible values of the Z' couplings allows to estimate the Z' production cross-section at the LHC and Tevatron and the Z' decay width without specifying the model beyond the SM.

3 Z' production cross-section

In modern experiments Z' bosons are expected to be produced in proton-antiproton collisions $p\bar{p} \rightarrow Z'$ (Tevatron) or proton-proton collisions $pp \rightarrow Z'$ (LHC). At the parton level both the processes are described by the annihilation of a quark-antiquark pair, $q\bar{q} \rightarrow Z'$ (Fig. 1). The Z' production cross-section is the result of integration of the partonic cross-section $\sigma_{q\bar{q} \rightarrow Z'}$ with the parton distribution functions:

$$\begin{aligned} \sigma_{AB} &= \sum_{q,\bar{q}} \int_0^1 dx_q \int_0^1 dx_{\bar{q}} f_{q,A}(x_q, Q^2) f_{\bar{q},B}(x_{\bar{q}}, Q^2) \\ &\times \sigma_{q\bar{q} \rightarrow Z'}(m_{Z'}, x_q k_A, x_{\bar{q}} k_B), \end{aligned} \quad (11)$$

where A, B mark the interacting hadrons (p or \bar{p}) with the four-momenta k_A, k_B ; $f_{q,A}$ is the parton distribution function for the parton q in the hadron A with the momentum fraction x_q ($0 \leq x_q \leq 1$) at the energy scale Q^2 . In our case $Q^2 = m_{Z'}^2$. We use the parton distribution functions provided by the MSTW PDF package [12].

The production cross-section is determined by quadratic combinations of the Z' couplings to quarks,

$$\begin{aligned} \sigma_{AB} &= \bar{a}^2 \sigma_{\bar{a}^2} + \bar{a} \bar{v}_u \sigma_{\bar{a} \bar{v}_u} + \bar{v}_u^2 \sigma_{\bar{v}_u^2} + \bar{a} \bar{v}_c \sigma_{\bar{a} \bar{v}_c} \\ &+ \bar{v}_c^2 \sigma_{\bar{v}_c^2} + \bar{a} \bar{v}_t \sigma_{\bar{a} \bar{v}_t} + \bar{v}_t^2 \sigma_{\bar{v}_t^2}. \end{aligned} \quad (12)$$

where relations (4)–(6) are taken into account. The factors σ depend on $m_{Z'}$, the process type (proton-proton or proton-antiproton collision), and the beam energy. The factors $\sigma_{\bar{a} \bar{v}_c}$, $\sigma_{\bar{v}_c^2}$, $\sigma_{\bar{a} \bar{v}_t}$ and $\sigma_{\bar{v}_t^2}$ are small compared to $\sigma_{\bar{a}^2}$, $\sigma_{\bar{a} \bar{v}_u}$ and $\sigma_{\bar{v}_u^2}$ and their contributions to the cross-section can be neglected.

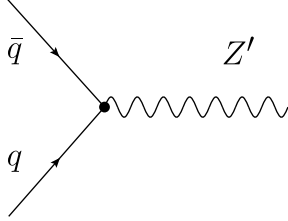


Figure 1: Z' production at the parton level.

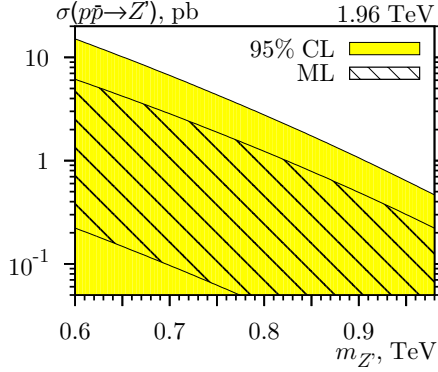


Figure 2: Z' production cross-section vs. $m_{Z'}$ in $p\bar{p}$ collisions at $\sqrt{S} = 1.96$ TeV. The filled area corresponds to the 95% CL estimate, and the hatched area is for the ML estimate.

We take into account the 90% CL uncertainties of the parton distribution functions provided by the MSTW PDF package. Finally, the production cross-section reads:

$$\begin{aligned}\sigma &= \bar{a}^2 \sigma_{\bar{a}^2} + \bar{a} \bar{v}_u \sigma_{\bar{a} \bar{v}_u} + \bar{v}_u^2 \sigma_{\bar{v}_u^2} \pm \Delta \sigma^{\text{pdf}}, \\ \Delta \sigma^{\text{pdf}} &= \bar{a}^2 \Delta \sigma_{\bar{a}^2}^{\text{pdf}} + \bar{a} \bar{v}_u \Delta \sigma_{\bar{a} \bar{v}_u}^{\text{pdf}} + \bar{v}_u^2 \Delta \sigma_{\bar{v}_u^2}^{\text{pdf}}.\end{aligned}\quad (13)$$

Due to the existence of the ML value for the axial-vector coupling we perform two different estimates for the production cross-section:

- *95% CL estimate.* In this scheme both the couplings \bar{a} and \bar{v}_u are varied in their 95% CL intervals (8), (10). Then the production cross-section lies inside of the interval between zero and some maximal value. The maximal value is reached when both the couplings \bar{a} and \bar{v}_u are of the same sign and take their maximal values: $\bar{a} = \sqrt{3.61} \times 10^{-2}$, $\bar{v}_u = 0.02$. The uncertainty from the parton distribution functions should be also added. This estimate leads to the widest interval of possible values of the production cross-section.
- *Maximum-likelihood estimate.* In this approach the axial-vector coupling is substituted by its ML value $\bar{a} = \sqrt{1.3} \times 10^{-5}$. The vector coupling \bar{v}_u is varied in its 95% CL interval. If one chooses the positive value of the axial-vector coupling, then the minimal value of the cross-section corresponds to $\bar{v}_u \simeq -0.02$ whereas the maximal value is reached at $\bar{v}_u \simeq 0.02$. The obtained interval should be also enlarged by $\Delta \sigma^{\text{pdf}}$. This estimate gives a more narrow interval for the production cross-section which can be considered as an ‘optimistic’ scenario to discover the Z' boson.

The estimates for the Z' production cross-section in proton-antiproton collisions at the Tevatron and in proton-proton collisions at the LHC are shown in Figs. 2 and 3, respectively. In the LHC case the \sqrt{S} value is taken to be 7 TeV

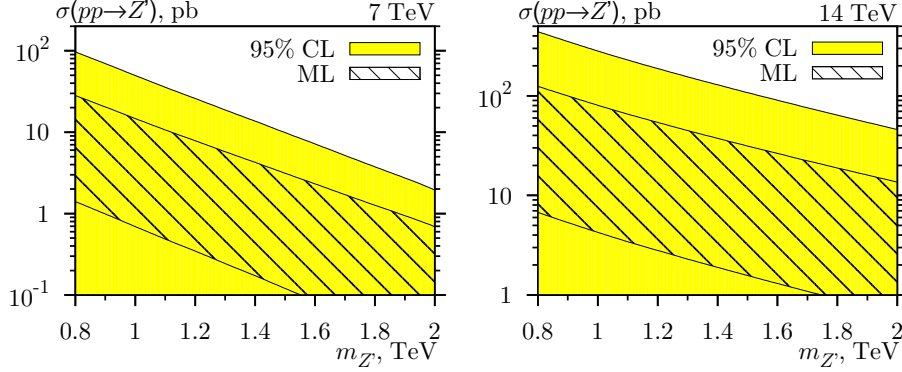


Figure 3: Z' production cross-section vs. $m_{Z'}$ in pp collisions at $\sqrt{S} = 7$ TeV and $\sqrt{S} = 14$ TeV. The filled area corresponds to the 95% CL estimate, and the hatched area is for the ML estimate.

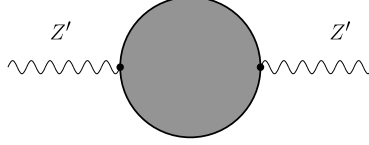


Figure 4: One-particle-irreducible correction to $Z' \rightarrow Z'$.

and 14 TeV, corresponding to the current and expected energies. The Z' mass is chosen to be from 600 to 980 GeV for the Tevatron process and from 800 to 2000 GeV for the LHC processes. At these masses it is possible to perform direct searches, and the boson production rate is not suppressed by the parton density effects.

4 Z' width

The Z' decay width $\Gamma_{Z'}$ can be calculated by using the optical theorem:

$$\Gamma_{Z'} = -\frac{\text{Im} G(m_{Z'}^2)}{m_{Z'}}, \quad (14)$$

where $G(p^2)$ is the two-point one-particle-irreducible Green's function corresponding to the diagram in Fig. 4. We compute $\Gamma_{Z'}$ at the one-loop level with the help of the FeynArts, FormCalc and LoopTools software [13, 14]. The Feynman diagrams with internal Z' lines as well as the Passarino-Veltman integrals of type A give no contribution to the result, since they are real. The rest of diagrams correspond to different channels of Z' decay. As a result, we obtain also all the partial widths corresponding to Z' decays into two SM particles.

All the Z' couplings to the SM scalar and vector bosons can be determined by the universal axial-vector constant a_f and can be constrained. Then the partial widths corresponding to Z' decays into scalar and vector bosons are proportional to a_f^2 . As for the fermionic decays, the width can be written in the

form

$$\Gamma_{Z' \rightarrow \bar{f} f} = a_f^2 \Gamma_{a_f^2} + a_f v_f \Gamma_{a_f v_f} + v_f^2 \Gamma_{v_f^2}. \quad (15)$$

The factors $\Gamma_{a_f^2}$, $\Gamma_{a_f v_f}$ and $\Gamma_{v_f^2}$ are proportional to $m_{Z'}$. Expressing eq. (15) through the constants (3) one can see that the width is proportional to $m_{Z'}^3$, and quadratic combinations of couplings \bar{a} , \bar{v}_f . Thus it is convenient to introduce quantity

$$\tilde{\Gamma} = \Gamma_{Z'} \times \left(\frac{1 \text{ TeV}}{m_{Z'}} \right)^3, \quad (16)$$

which is independent of $m_{Z'}$ in our estimates.

To calculate $\tilde{\Gamma}$ numerically one has to choose values of the unknown masses of the SM scalar particles. If the minimal SM is considered as the low-energy theory, the only unknown mass is the Higgs boson mass m_h . The modern constraints on its value indicate that it is quite heavy, $m_h \geq 114 \text{ GeV}$. The contribution to the decay width from the scalar sector appears to be two or three orders of magnitude lower than the leading contribution from the fermionic decay channel. So the decay widths calculated at different values of m_h are practically indistinguishable. In this regard, we present the results obtained for $m_h = 125 \text{ GeV}$.

When the THDM is considered, the scalar sector has six free parameters that can be expressed in terms of the masses m_h , m_H , m_{A_0} , m_{H^\pm} and the mixing angles $\tan \alpha$, $\tan \beta$ (see Appendix A for details). Because of the large number of physical scalar fields the estimates for the Z' width within the THDM can deviate from the results obtained in the case of the minimal SM. In order to obtain the most significant difference, we choose H^\pm and A_0 to be as light as it is allowed by the LEP constraints [15], namely

$$m_{H^\pm} = 81 \text{ GeV}, \quad m_{A_0} = 92 \text{ GeV}. \quad (17)$$

The h and H masses are set to

$$m_h = m_H = 125 \text{ GeV} \quad (18)$$

just like in the SM case. The dependence of $\tilde{\Gamma}$ on the mixing angles is negligibly weak. We take $\tan \beta = 2$, which respects the LEP constraints. The $\tan \alpha$ value is set to 0.75.

The decay width is estimated in two schemes which are similar to the case of the production cross-section:

- *95% CL estimate.* In this scheme the coupling constants \bar{a} and \bar{v}_f are varied in their 95% CL intervals (8), (10). The minimal value of the width is calculated at $\bar{a} = \bar{v}_u = \bar{v}_{\mu, \tau} = 0$, $\bar{v}_e = \pm \sqrt{0.4} \times 10^{-2}$. The maximal value is realized when all the couplings are at their maximal absolute values, \bar{a} and $\bar{v}_{u, c, t}$ are of the same sign, while $\bar{v}_{e, \mu, \tau}$ have the opposite sign with respect to \bar{a} : $\bar{a} = \pm \sqrt{3.61} \times 10^{-2}$, $\bar{v}_{u, c, t} = \pm 0.02$, $\bar{v}_{\mu, \tau} = \mp 0.02$, $\bar{v}_e = \mp \sqrt{1.69} \times 10^{-2}$.
- *Maximum-likelihood estimate.* We set $\bar{a} = \sqrt{0.13} \times 10^{-2}$ and vary v_f in their 95% CL intervals. We choose the positive value of \bar{a} , so the minimum value of the width corresponds to $\bar{v}_e = \sqrt{0.4} \times 10^{-2}$ and $\bar{v}_f = -\bar{a}_f \tilde{\Gamma}_{\bar{a}_f \bar{v}_f} / 2 \tilde{\Gamma}_{\bar{v}_f^2}$ ($f = \mu, \tau, u, c, t$). The maximum value is reached at $\bar{v}_{u, c, t} = 0.02$, $\bar{v}_{\mu, \tau} = -0.02$, $\bar{v}_e = -\sqrt{1.69} \times 10^{-2}$.

The Z' width (16) is plotted in Fig. 5 as the function of \bar{v}_e . The minimal SM and the THDM lead to slightly different bounds depicted in Fig. 6.

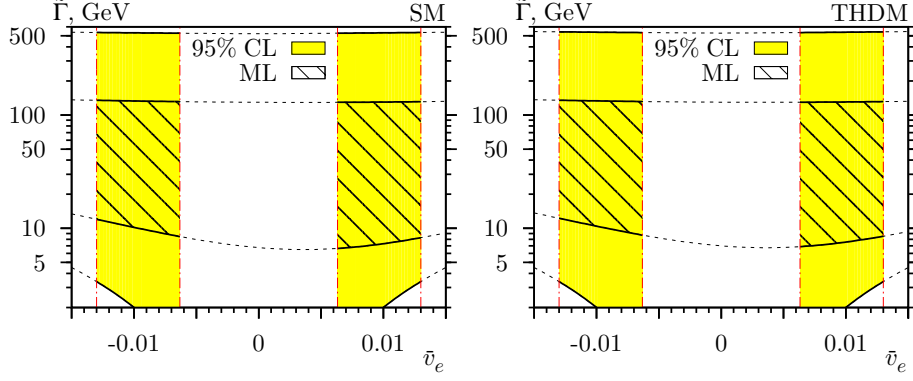


Figure 5: The Z' width (16) versus \bar{v}_e for the SM and THDM cases. The filled areas represent the 95% CL estimate, whereas the hatched areas represent the ML estimate. The inner vertical dot-dashed lines stand for the minimum 95% CL value of \bar{v}_e from the special one-parameter fit of the LEP II data, the outer ones depict the maximum 95% CL value of \bar{v}_e from the general two-parameter fit of the LEP II data.

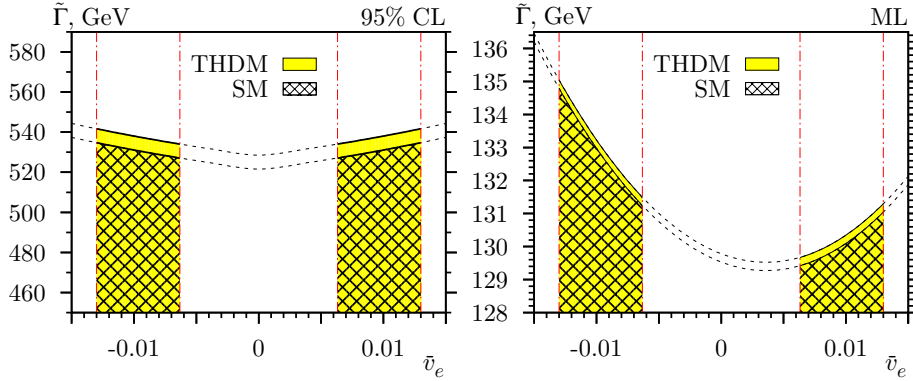


Figure 6: The $\tilde{\Gamma}$ estimates versus \bar{v}_e for the SM and THDM cases. The filled areas represent the estimate for the THDM case, and the hatched areas represent the estimate for the SM case. The meaning of the vertical dot-dashed lines is the same as in Fig. 5.

Since we chose the positive ML value of the axial-vector coupling \bar{a} , we obtain asymmetric domain in the parameter space within the ML estimate as it is seen in Figs. 5 and 6. This asymmetry arises from the term $\bar{a}\bar{v}_e\Gamma_{\bar{a}\bar{v}_e}$ in (15). Of course, the sign of \bar{a} is not constrained by the experimental data, so the sign of the vector coupling should be considered as the relative sign with respect to the axial-vector coupling. For the electron vector coupling the 2σ hint was observed [10]. This allows to exclude the area near $\bar{v}_e = 0$ shown in the figures.

Consider an example of usage of the obtained estimates. Let us assume that

the Z' mass is of order 1–2 TeV, for instance $m_{Z'} = 1.5$ TeV, so Z' production rate in the LHC and Tevatron processes is non-negligible and the direct searches are possible. The ML value $\tilde{\Gamma} \approx 50$ GeV leads to the total decay width $\Gamma_{Z'} = 169$ GeV. Thus we can expect the Z' resonance compatible with the narrow width approximation (NWA), $\Gamma_{Z'}^2/m_{Z'}^2 = 0.013 \ll 1$. However, one has to keep in mind that $\Gamma_{Z'} \approx m_{Z'}$ is not excluded at the 95% CL. The extremely narrow resonances with $\Gamma_{Z'} \approx 1$ GeV are also not excluded.

It is also useful to estimate the partial decay widths of the Z' boson. In this analysis we take the ML value of the axial-vector coupling $\bar{a} = \sqrt{0.13} \times 10^{-2}$ and vary other couplings in their 95% CL intervals. The results are presented as the plots in which a partial width is depicted versus the total width. In this way the branching ratios can be easily obtained.

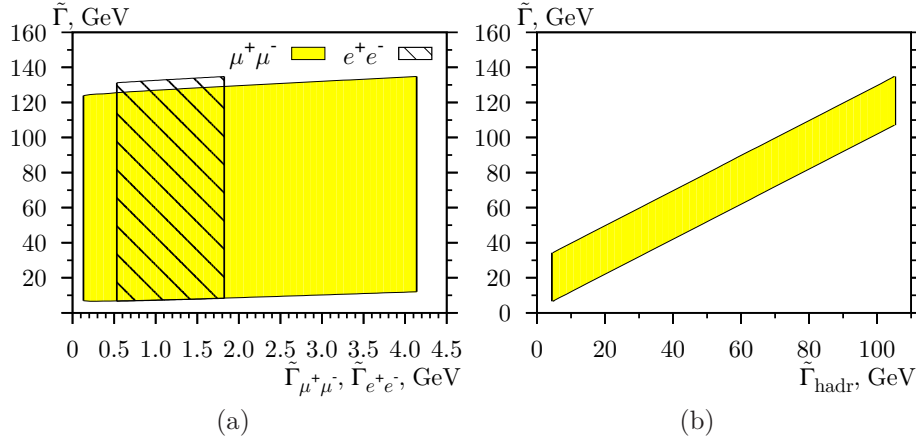


Figure 7: (a) The ML estimates on the $\tilde{\Gamma}$ versus $\tilde{\Gamma}_{e^+e^-}$ and $\tilde{\Gamma}_{\mu^+\mu^-}$ plane. The filled area is for dimuon channel, and the hatched area represents the dielectron channel. (b) The ML domain on the $\tilde{\Gamma}$ – $\tilde{\Gamma}_{\text{hadr}}$ plane.

The partial decay widths for the electron-positron, muon-antimuon, and quark-antiquark channels are shown in Fig. 7. On these plots, the difference between the SM and the THDM case is negligible. As it is seen, the branching ratio for the electron-positron decay channel can be expected in the wide interval

$$0.004 \leq BR(Z' \rightarrow e^+e^-) \leq 0.21. \quad (19)$$

Here, the minimal value corresponds to $\bar{v}_e = 0$, whereas the maximal value is reached at $\bar{v}_e = -\sqrt{1.69} \times 10^{-2}$. The significant difference between the estimates for $\tilde{\Gamma}_{e^+e^-}$ and $\tilde{\Gamma}_{\mu^+\mu^-}$ is caused by the fact that the Z' vector coupling to electron is much better constrained by the LEP II data than the muon one. The decay into quark-antiquark pairs can be the dominant decay channel. The corresponding probability can amount to 98%.

Considering the Z' partial widths, one can find a significant distinction between the SM and THDM in the scalar sector. Since \bar{a} is the only Z' coupling entering the scalar and vector contributions to $\Gamma_{Z'}$, there is the ML value of the partial decay width into two SM bosons (vectors or scalars). In the SM case, $\tilde{\Gamma}_{\text{bosons}} = 0.27$ GeV. In the THDM case, $\tilde{\Gamma}_{\text{bosons}} = 0.53$ GeV. The corresponding branching ratios are less than 2.5%.

5 Discussion

The recent experiments at the LEP gave some hints of the Abelian Z' boson. Although these hints correspond to 68-95% CL, they can be used as a beacon showing the most optimistic scenario to find Z' boson with a mass near 1 TeV. It is interesting to speculate about the question how can those hints look like at Tevatron and LHC experiments. Taking the LEP ML value of the axial-vector coupling we can give predictions under the assumption that a signal of the Abelian Z' boson has been probably observed in the LEP data. This estimate, called ML scheme, represents the most bold expectations concerning the Abelian Z' boson. Of course, such predictions do not exclude Z' boson with weaker axial-vector couplings.

On the other hand the 95% CL bounds on possible Z' couplings to the SM particles are left behind the LEP experiments. Taking these bounds for all the Z' couplings we can exclude some values of the observables at hadron colliders. In this scheme the values outside of the predicted intervals are forbidden for the Abelian Z' boson. Being measured in experiments, such values have to be interpreted as a signal of new physics which is something else than the Z' boson. For example, considering the Z' width, we can expect $\Gamma_{Z'} \times (1 \text{ TeV}/m_{Z'})^3 \simeq 10 - 150 \text{ GeV}$ from the ML estimate, and we can think about the NWA for $m_{Z'} \leq 2 \text{ TeV}$. On the other hand, only extremely narrow resonances, $\Gamma_{Z'} \times (1 \text{ TeV}/m_{Z'})^3 < 1 \text{ GeV}$, and extremely wide resonances, $\Gamma_{Z'} \times (1 \text{ TeV}/m_{Z'})^3 > 500 \text{ GeV}$, can be surely excluded at the 95% CL. Thus, waiting for a narrow Z' resonance at hadron colliders we have to keep in mind that a more rich Z' phenomenology is still allowed by existing data.

Now let us present the ML estimate for the Drell-Yan cross-section for the Tevatron and LHC experiments. As it was mentioned, in this case the NWA can be applied and the Z' contribution to the cross-section of the $pp(p\bar{p}) \rightarrow l\bar{l}$ process reads $\sigma(pp(p\bar{p}) \rightarrow Z') \times BR(Z' \rightarrow l\bar{l})$ where the branching ratio can be extracted from the total and partial Z' decay widths. The experimental bounds on the Z' contribution to the Drell-Yan process at the Tevatron are available in [16, 17, 18] together with the predictions from popular Z' models. The comparison between those results and our ML estimate for $\sigma(p\bar{p} \rightarrow Z' \rightarrow e^+e^-, \mu^+\mu^-)$ is presented in Figs. 8. We can conclude from both the D0 and CDF limits that the Z' hints from the LEP data can be the Abelian Z' boson with the mass between 400 GeV and 1.2 TeV. Our model-independent results cover all the popular Z' models. We can also conclude that the model-independent lower bound on the Z' mass is still about 400 GeV whereas the popular models give the lower bound of order 800 – 900 GeV.

It is straightforward to carry out similar calculations for $pp \rightarrow Z' \rightarrow l^+l^-$ processes at the LHC. The ML domains are presented in Figs. 9. The cross-section values are plotted for the Z' mass up to 2 TeV. For higher masses the validity of the NWA is not guaranteed even for the ML estimate. Let us compare the results to the ones presented in [19]. In Fig. 3 of Ref. [19] the number of $pp \rightarrow Z' \rightarrow l^+l^-$ events for 100 fb⁻¹ of integrated luminosity at $\sqrt{S} = 14 \text{ TeV}$ versus $m_{Z'}$ is plotted. The ML number of $pp \rightarrow Z' \rightarrow e^+e^-$ or $\mu^+\mu^-$ events for this luminosity can be obtained by multiplying the cross-section values in the left plot in Fig. 9 by 10⁵. It can be seen that all the model-dependent predictions from Ref. [19] are covered by the e^+e^- ML domain.

In Table 2 of Ref. [19] the model-dependent estimates for $\sigma(pp \rightarrow Z' \rightarrow$

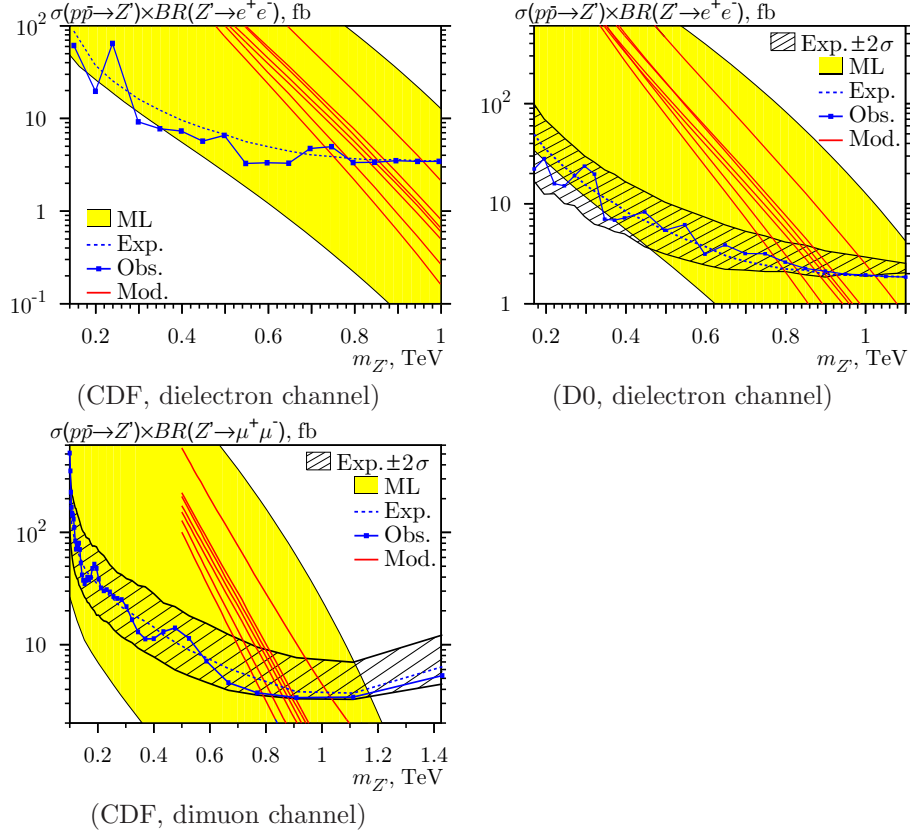


Figure 8: The comparison between the Tevatron results and the ML estimates of the Z' production in the Drell-Yan process at $\sqrt{S} = 1.96$ TeV. In all plots the filled areas represent the ML estimates. The experimentally obtained upper limits on the Z' contribution are taken from [16, 17, 18]: the expected and observed 95% CL upper limits are depicted by the dashed lines and line charts, respectively, and the hatched areas are the 2σ standard deviation bands for the expected values. The predictions from the popular models [16, 17, 18] are plotted as solid red lines, the corresponding models are Z'_1 , Z'_{sec} , Z'_N , Z'_ψ , Z'_χ , Z'_η and SSM Z' from the left to the right.

$l^+l^-) \times \Gamma_{Z'}$ are presented. $m_{Z'}$ is set to 1.5 TeV. The ML estimate for this observable is easy to calculate using Figs. 3 and 7 (a) as $\sigma(pp \rightarrow Z') \times \tilde{\Gamma}^{l^+l^-} \times (m_{Z'}/1 \text{ TeV})^3$. We obtain $94 \pm 92 \text{ pb} \cdot \text{GeV}$ and $210.7 \pm 210.1 \text{ pb} \cdot \text{GeV}$ for e^+e^- and $\mu^+\mu^-$ decay channels, respectively. One can see that the predictions for the Z'_ψ and Z'_η models ($487 \pm 5 \text{ fb} \cdot \text{GeV}$ and $630 \pm 20 \text{ fb} \cdot \text{GeV}$) lie outside the ML interval for the dielectron channel case, and the Z'_ψ prediction is not covered by the dimuon channel estimate. This is because $m_{Z'} = 1.5 \text{ TeV}$ appears to be quite heavy to provide exact value of the axial-vector coupling from the LEP data as it is assumed in the ML scheme. Of course, the model-dependent results are covered by the 95% CL intervals and cannot be excluded by the LEP data.

The model-independent relations for the Z' couplings give a good possibility to reduce the number of unknown Z' parameters. As a consequence, the Z'

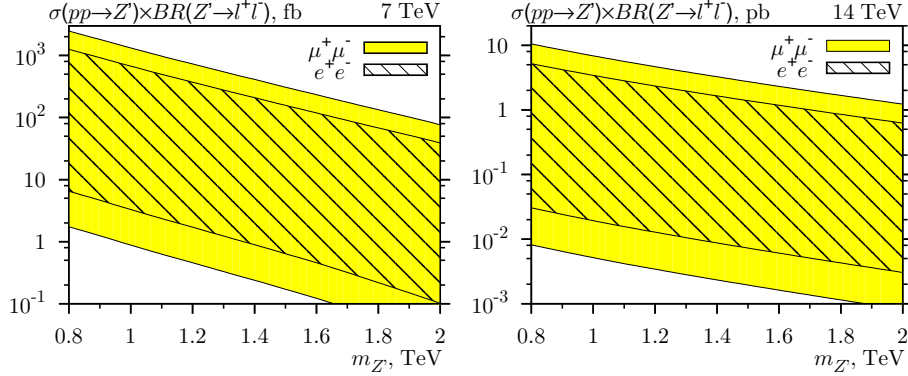


Figure 9: The ML domain for $\sigma(pp \rightarrow Z') \times BR(Z' \rightarrow e^+e^-)$ (hatched area) and $\sigma(pp \rightarrow Z') \times BR(Z' \rightarrow \mu^+\mu^-)$ (filled area) at $\sqrt{S} = 7$ TeV and 14 TeV.

width and the production cross-sections of the processes at modern hadron colliders can be estimated using the constraints on the Z' couplings obtained from previous experiments at LEP. A combined analysis of the LEP, Tevatron and LHC data seems to be possible.

Our new model-independent results are complementary to the usual model-dependent schemes. The predictions of all the popular Z' models agree with our model-independent bounds.

Finally the Z' hints observed in the LEP data can be still hidden as the resonance in the Tevatron experiments. We can expect this Z' boson with the mass between 400 GeV and 1.2 TeV.

A Lagrangian

In this section we adduce the scalar, fermion, Yukawa and gauge sectors of the Lagrangian that is used for the calculations.

Let ϕ_i ($i = 1, 2$) be two complex scalar doublets:

$$\phi_i^T = \left\{ a_i^+, \frac{v_i + b_i + ic_i}{\sqrt{2}} \right\}, \quad (20)$$

where v_i marks corresponding vacuum expectation values, a_i^+ are complex fields, and b_i , c_i are real fields. By diagonalizing the quadratic terms of the scalar potential $V(\phi_1, \phi_2)$ one obtains the mass eigenstates: two neutral CP -even scalar particles, H and h , the neutral CP -odd scalar particle, A_0 , the Goldstone boson partner of the Z boson, χ_3 , the charged Higgs field, H^\pm , and the Goldstone field associated with the W^\pm boson, χ^\pm :

$$\begin{aligned} a_1^+ &= \chi^+ \cos \beta - H^+ \sin \beta, & a_2^+ &= H^+ \cos \beta + \chi^+ \sin \beta, \\ c_1 &= \chi_3 \cos \beta - A_0 \sin \beta, & c_2 &= A_0 \cos \beta + \chi_3 \sin \beta, \\ b_1 &= H \cos \alpha - h \sin \alpha, & b_2 &= h \cos \alpha + H \sin \alpha, \end{aligned} \quad (21)$$

where

$$\tan \beta = \frac{v_2}{v_1}, \quad (22)$$

and the angle α is determined by the explicit form of the potential $V(\phi_1, \phi_2)$. For instance, the CP -conserving potential, which has only CP -invariant minima, can be used [24, 25]:

$$V = \sum_{i=1}^2 \left[-\mu_i^2 \phi_i^\dagger \phi_i + \lambda_i (\phi_i^\dagger \phi_i)^2 \right] + \lambda_3 (\text{Re}[\phi_1^\dagger \phi_2])^2 + \lambda_4 (\text{Im}[\phi_1^\dagger \phi_2])^2 + \lambda_5 (\phi_1^\dagger \phi_1)(\phi_2^\dagger \phi_2). \quad (23)$$

It is consistent with the absence of the tree-level flavor-changing neutral currents (FCNC's) in the fermion sector. The corresponding value of α is [25]

$$\tan 2\alpha = -\frac{v_1 v_2 (\lambda_3 + \lambda_5)}{\lambda_2 v_2^2 - \lambda_1 v_1^2}. \quad (24)$$

The Z' coupling to the scalar doublets can be parametrized in a model independent way as follows [22]:

$$\mathcal{L}_\phi = \sum_{i=1}^2 \left| \left(\partial_\mu - \frac{ig}{2} \sigma_a W_\mu^a - \frac{ig'}{2} Y_{\phi_i} B_\mu - \frac{i\tilde{g}}{2} \tilde{Y}_{\phi_i} \tilde{B}_\mu \right) \phi_i \right|^2, \quad (25)$$

where g , g' , \tilde{g} are the charges associated with the $SU(2)_L$, $U(1)_Y$, and the Z' gauge groups, respectively, σ_a are the Pauli matrices,

$$\tilde{Y}_{\phi_i} = \begin{pmatrix} \tilde{Y}_{\phi_i,1} & 0 \\ 0 & \tilde{Y}_{\phi_i,2} \end{pmatrix} \quad (26)$$

is the generator corresponding to the gauge group of the Z' boson, and Y_{ϕ_i} is the $U(1)_Y$ hypercharge. The condition $Y_{\phi_i} = 1$ guarantees that the vacuum is invariant with respect to the gauge group of photon.

The vector bosons, A , Z , and Z' , are related with the symmetry eigenstates as follows:

$$\begin{aligned} B &\rightarrow A \cos \theta_W - (Z \cos \theta_0 - Z' \sin \theta_0) \sin \theta_W, \\ W_3 &\rightarrow A \sin \theta_W + (Z \cos \theta_0 - Z' \sin \theta_0) \cos \theta_W, \\ \tilde{B} &\rightarrow Z \sin \theta_0 + Z' \cos \theta_0, \end{aligned} \quad (27)$$

where $\tan \theta_W = g'/g$ is the adopted in the SM value of the Weinberg angle, and

$$\tan \theta_0 = \frac{\tilde{g} m_W^2 (\tilde{Y}_{\phi_1,2} \cos^2 \beta + \tilde{Y}_{\phi_2,2} \sin^2 \beta)}{g \cos \theta_W (m_{Z'}^2 - m_W^2 / \cos^2 \theta_W)}. \quad (28)$$

As is seen, the mixing angle θ_0 is of order $\sim m_W^2/m_{Z'}^2$. That results in the corrections of order $\sim m_W^2/m_{Z'}^2$ to the interactions between the SM particles. To avoid the tree-level mixing of the Z boson and the physical scalar field A_0 one has to impose the condition $\tilde{Y}_{\phi_1,2} = \tilde{Y}_{\phi_2,2} \equiv \tilde{Y}_{\phi,2}$.

The effective low-energy Lagrangian of the fermion-vector interactions reads [20, 21, 22]:

$$\begin{aligned} \mathcal{L}_f &= i \sum_{f_L} \bar{f}_L \gamma^\mu \left(\partial_\mu - \frac{ig}{2} \sigma_a W_\mu^a - \frac{ig'}{2} B_\mu Y_{f_L} - \frac{i\tilde{g}}{2} \tilde{B}_\mu \tilde{Y}_{f_L} \right) f_L \\ &+ i \sum_{f_R} \bar{f}_R \gamma^\mu \left(\partial_\mu - ig' B_\mu Q_f - \frac{i\tilde{g}}{2} \tilde{B}_\mu \tilde{Y}_{R,f} \right) f_R, \end{aligned} \quad (29)$$

where the renormalizable type interactions are admitted and the summation over the all SM left-handed fermion doublets, $f_L = \{(f_u)_L, (f_d)_L\}$, and the right-handed singlets, $f_R = (f_u)_R, (f_d)_R$, is understood. Q_f denotes the charge of f in the positron charge units,

$$\tilde{Y}_{f_L} = \begin{pmatrix} \tilde{Y}_{L,f_u} & 0 \\ 0 & \tilde{Y}_{L,f_d} \end{pmatrix}, \quad (30)$$

and Y_{f_L} equals to -1 for leptons and $1/3$ for quarks.

In the present paper we use the Z' couplings to the vector and axial-vector fermion currents defined as

$$v_f = \tilde{g} \frac{\tilde{Y}_{L,f} + \tilde{Y}_{R,f}}{2}, \quad a_f = \tilde{g} \frac{\tilde{Y}_{R,f} - \tilde{Y}_{L,f}}{2}. \quad (31)$$

The Lagrangian (29) leads to the interactions between the fermions and the Z and Z' mass eigenstates described by (1).

Renormalizable interactions of fermions and scalars are described by the Yukawa Lagrangian. To avoid the existence of the tree-level FCNC's one has to ensure that at the diagonalization of the fermion mass matrix the diagonalization of the scalar-fermion couplings is automatically fulfilled. In this case the Yukawa Lagrangian, which respects the $SU(2)_L \times U(1)_Y$ gauge group, can be written in the form:

$$\begin{aligned} \mathcal{L}_{\text{Yuk}} = & -\sqrt{2} \sum_{f_L} \sum_{i=1}^2 \left\{ G_{f_d,i} \left[\bar{f}_L \phi_i (f_d)_R + (\bar{f}_d)_R \phi_i^\dagger f_L \right] \right. \\ & \left. + G_{f_u,i} \left[\bar{f}_L \phi_i^c (f_u)_R + (\bar{f}_u)_R \phi_i^{c\dagger} f_L \right] \right\}, \end{aligned} \quad (32)$$

where $\phi_i^c = i\sigma_2 \phi_i^*$ is the charge conjugated scalar doublet, and the Cabibbo-Kobayashi-Maskawa mixing is neglected. Then, the fermion masses are

$$m_f = \frac{2m_W}{g} (G_{f,1} \cos \beta + G_{f,2} \sin \beta). \quad (33)$$

As was shown by Glashow and Weinberg [26], the tree-level FCNC's mediated by Higgs bosons are absent in case when all fermions of a given electric charge couple to no more than one Higgs doublet. This restriction leads to four different models, as discussed in Ref. [25]. In what follows, we will use the most general parametrization (32) including the models mentioned as well as other possible variations of the Yukawa sector without the tree-level FCNC's.

The gauge sector is taken to be

$$\mathcal{L}_{\text{gauge}} = -\frac{1}{4} F^{\mu\nu} F_{\mu\nu} - \frac{1}{4} F_a^{\mu\nu} F_{\mu\nu}^a - \frac{1}{4} \tilde{F}^{\mu\nu} \tilde{F}_{\mu\nu}. \quad (34)$$

In the present paper all calculations are carried out in the Feynman-'t Hooft gauge, the gauge-fixing functions are

$$\begin{aligned} G^a &= \frac{1}{\sqrt{\xi}} \left(\partial^\mu A_\mu^a + \xi \frac{ig}{2} \sum_{i=1}^2 \left(\varphi_i^\dagger \sigma^a \varphi_{0i} - \varphi_{0i}^\dagger \sigma^a \varphi_i \right) \right), \\ G &= \frac{1}{\sqrt{\xi}} \left(\partial^\mu B_\mu + \xi \frac{ig'}{2} \sum_{i=1}^2 \left(\varphi_i^\dagger \varphi_{0i} - \varphi_{0i}^\dagger \varphi_i \right) \right), \end{aligned}$$

$$\begin{aligned}\tilde{G} &= \frac{1}{\sqrt{\xi}} \left(\partial^\mu \tilde{B}_\mu + \xi \frac{i\tilde{g}}{2} \sum_{i=1}^2 \left(\varphi_i^\dagger \varphi_{0i} - \varphi_{0i}^\dagger \varphi_i \right) \right), \\ \varphi_{0i} &= \begin{pmatrix} 0 \\ v_i/\sqrt{2} \end{pmatrix}.\end{aligned}\tag{35}$$

Then, the gauge-fixing part of the Lagrangian reads

$$\mathcal{L}_{\text{gauge fixing}} = -\frac{1}{2} \left(\sum_{a=1}^3 G^{a2} + G^2 + \tilde{G}^2 \right).\tag{36}$$

The kinetic part of Faddeev-Popov sector is

$$\begin{aligned}\mathcal{L}_{\text{ghost}} &= -\bar{u}^+(\partial^2 + \xi m_W^2)u^- - \bar{u}^-(\partial^2 + \xi m_W^2)u^+ \\ &\quad -\bar{u}_Z(\partial^2 + \xi m_Z^2)u_Z - \bar{u}_A\partial^2 u_A \\ &\quad -\bar{u}_{Z'}(\partial^2 + \xi m_{Z'}^2)u_{Z'},\end{aligned}\tag{37}$$

ξ is gauge-fixing parameter. For arbitrary ξ the gauge-boson propagator is

$$iD^{\mu\nu}(p) = -\frac{i}{p^2 - m^2 + i\epsilon} \left(g^{\mu\nu} + (\xi - 1) \frac{p^\mu p^\nu}{p^2 - \xi m^2} \right).\tag{38}$$

The MSM parametrization can be obtained by putting $\tan\beta$, $\tan\alpha$, μ_2 , $\lambda_{2,3,4,5}$, $\tilde{Y}_{\phi_{2,1,2}}$, $G_{d,2}$ and $G_{u,2}$ to zero and dropping the summations over i in (25), (32) and (35).

In Refs. [7, 8] the relations between Z' parameters were found from the requirement that the underlying extended model is a renormalizable one. They read

$$\tilde{Y}_{\phi,1} = \tilde{Y}_{\phi,2} \equiv \tilde{Y}_\phi, \quad \tilde{Y}_{L,f} = \tilde{Y}_{L,f^*}, \quad \tilde{Y}_{R,f} = \tilde{Y}_{L,f} + 2T_{3f} \tilde{Y}_\phi\tag{39}$$

in case of Abelian Z' boson. Here f and f^* are the partners of the $SU(2)_L$ fermion doublet ($l^* = \nu_l, \nu^* = l, q_u^* = q_d$ and $q_d^* = q_u$), T_{3f} is the third component of weak isospin. These relations are used all over the present paper. They can be also rewritten in terms of vector couplings, axial-vector couplings, and the Z - Z' mixing angle.

References

- [1] A. Leike, *Phys. Rep.* **317**, 143 (1999).
- [2] P. Langacker, *Rev. Mod. Phys.* **81**, 1199-1228 (2008); e-print arXiv:0801.1345 [hep-ph].
- [3] T. Rizzo, e-print hep-ph/0610104.
- [4] J. Erler, P. Langacker, S. Munir and E. R. Pena, *JHEP* **08**, 017 (2009).
- [5] F. del Aguila, J. de Blas and M. Perez-Victoria, e-print arXiv:1005.3998.
- [6] J. Erler, P. Langacker, S. Munir, E. Rojas, e-print arXiv:1010.3097v1 [hep-ph]

- [7] A. V. Gulov and V. V. Skalozub, *Eur. Phys. J. C* **17**, 685 (2000).
- [8] A. V. Gulov and V. V. Skalozub, *Phys. Rev. D* **61**, 055007 (2000).
- [9] A. V. Gulov and V. V. Skalozub, e-print arXiv:0905.2596v2 [hep-ph].
- [10] A. V. Gulov and V. V. Skalozub, *Int. J. Mod. Phys. A* **25**, 5787-5815 (2010).
- [11] G. Altarelli et al., *Z. Phys. C* **45**, 109 (1989); erratum *Z. Phys. C* **47**, 676 (1990).
- [12] A.D. Martin, W.J. Stirling, R.S. Thorne and G. Watt, *Eur. Phys. J. C* **63**, 189 (2009); *ibid.* **64**, 653 (2009); *ibid.* **70**, 51 (2010); e-print arXiv:0901.0002v3 [hep-ph]; e-print arXiv:0905.3531v2 [hep-ph]; e-print arXiv:1007.2624v2 [hep-ph]; <http://projects.hepforge.org/mstwpdf/>.
- [13] T. Hahn, *Comput. Phys. Commun.* **140**, 418 (2001); e-print arXiv:hep-ph/0012260v2; <http://www.feynarts.de/>.
- [14] T. Hahn and M. Perez-Victoria, *Comput. Phys. Commun.* **118**, 153 (1999); e-print arXiv:hep-ph/9807565v1; <http://www.feynarts.de/formcalc/>, <http://www.feynarts.de/looptools/>.
- [15] K. Nakamura et al. (Particle Data Group), *J. Phys. G* **37**, 2010 (075021).
- [16] CDF Collaboration, T. Aaltonen et al., *Phys. Rev. Lett.* **102**, 031801 (2009), e-print arXiv:0810.2059.
- [17] CDF Collaboration, T. Aaltonen et al., *Phys. Rev. Lett.* **102**, 091805 (2009), e-print arXiv:0811.0053.
- [18] D0 Collaboration, V. Abazov, et al., *Phys. Lett. B* **695**, 88 (2011), e-print arXiv:1008.2023.
- [19] M. Dittmar, A. Djouadi and A.-S. Nicollrat, *Phys. Lett. B* **583**, 111 (2004), e-print arXiv:hep-ph/0307020v1.
- [20] G. Degrossi and A. Sirlin, *Phys. Rev. D* **40**, 3066 (1989).
- [21] C. Caso et al., *Eur. Phys. J. C* **3**, 1 (1998).
- [22] M. Cvetič and B. W. Lynn, *Phys. Rev. D* **35**, 51 (1987).
- [23] A. V. Gulov and V. V. Skalozub, *int. J. Mod. Phys. A* **16**, 179 (2001).
- [24] J. Gunion, H. Haber, G. Kane, and S. Dawson, *The Higgs Hunter's Guide* (Addison-Wesley, Reading, MA, 1990)
- [25] R. Santos and A. Barroso, *Phys. Rev. D* **56**, 5366 (1997).
- [26] S. Glashow and S. Weinberg, *Phys. Rev. D* **15**, 1958 (1977).